*The 2019 World Congress on*
***Advances in Nano, Bio, Robotics and Energy (ANBRE19)***
*Jeju Island, Korea, September 17 - 21, 2019*

# Experimental study of the pool spreading due to continuous release of cryogenic liquids

*Myungbae Kim[1)] and Le-Duy Nguyen[2)]

*[1), 2)] Department of Plant Technology, KIMM(UST), Daejeon 34103, Korea*
*[1)] mbkim@kimm.re.kr*

## ABSTRACT

The study of spread of cryogenic liquids is an essential procedure for assessing the risk of using cryogenic liquids. There are various numerical models for describing the spread of a liquid pool formed by leakage of a cryogenic liquid. Some models, such as the constant Froude number model and the shallow layer model, require the vaporization velocity as the input variable. The vaporization velocity should be determined experimentally because the heat transfer mechanism between the liquid pool and the surrounding is very complicated and difficult to model. In this study, liquid nitrogen and liquid oxygen were continuously discharged onto a 3 m diameter unbounded concrete plate to measure the vaporization velocity when the liquid pool was spreading. Since the concrete plate is heavy, it is impossible to simultaneously measure the radius of the pool using the thermocouple and the mass of the pool using the electronic scale. So only the spread radius of the pool was measured. Therefore, the vaporization velocity was evaluated based on the semi-analytical model using pool spread data. Various release rates were obtained using several nozzles, and the effect of the rates on the vaporization velocity was investigated.

## 1. INTRODUCTION

Cryogenic liquids such as liquefied hydrogen, liquefied natural gas, and liquid nitrogen are widely used, but accidents during storage or transportation can cause serious problems. When the cryogenic liquid leaks from the storage vessel and spreads in the outside, it takes the form of a liquid pool. Since the ambient temperature is usually much higher than the boiling temperature of the cryogenic liquid, the cryogenic liquid pool experiences vigorous boiling due to heat exchange with the environment. As a result, a vapor cloud is formed from the liquid pool heated by various heat sources. The main sources of heat are the heat from the ground, the convection heat from the ambient air, and the radiation from the sun. If the leaked cryogenic liquid is flammable, there is a clear possibility of pool fire and vapor cloud explosion. Furthermore, if the liquid is toxic, it may disperse into the atmosphere with the wind, and the perimeter of the leak may be dangerous. Therefore, studies on the spread and vaporization of cryogenic liquid pools are an important part of the risk assessment of cryogenic liquid

---

[1)] Professor
[2)] Graduate Student

storage facilities.

Several models have been proposed as a result of analytical solutions (Briscoe 1980, Kim 2012) and numerical analyzes (Verfondern 1997, Brandeis 1983, Stein 1980) to predict pool spread. Most of the models ignore radiative heat transfer and convective heat transfer, only considering conduction heat transfer from ground. An important element of these models is to omit the energy equation and the vaporization velocity equation of the liquid pool through the introduction of the vaporization velocity, i.e. the volume evaporated per unit area per unit time (Webber 1990). These equations are so complex that it is not easy to obtain a stable solution. Therefore, in all of the studies, the vaporization velocity was used as an input variable.

In many experiments to measure the vaporization velocity, the cryogenic liquid is poured instantaneously onto the bounded ground where spread is limited, so that the leak is in the form of an instantaneous release (American Petroleum Institute 2008) where the release time is much shorter than the vaporization time. In this non-spreading pool (Zabetakis 1960, Takeno 1994, Olewski 2013, Reid 1978), the ground surface temperature continuously decreases, and the heat flux due to conduction is also continuously reduced. Usually, the spread rate of the non-spreading pool in a bounded surface is not measured. In a real accident, the liquid pool will evaporate as it spreads because most of the cryogenic liquid will leak continuously over unbounded ground. Since the liquid pool spreads continuously over new high temperature surfaces, heat energy due to conduction can be received effectively more than the non-spreading pool. The measurement of the vaporization velocity in the spreading pool was performed mainly by the authors (Kim 2016, Nguyen 2017) and two measurement methods were developed. One is the simultaneous measurement of the spill rate and the mass and radius of the spreading pool, and the other is based on the semi-analytical method.

In this study, liquid nitrogen and liquid oxygen were continuously discharged onto a 3 m diameter unbounded concrete plate to measure the vaporization velocity when the liquid pool was spreading. Since the concrete plate is heavy, it is impossible to simultaneously measure the radius of the pool using the thermocouple and the mass of the pool using the electronic scale. So only the spread radius of the pool was measured. Therefore, the vaporization velocity was evaluated based on the semi-analytical model using pool spread data. Various release rates were obtained using several nozzles, and the effect of the rates on the vaporization velocity was investigated.

## 2. VAPORIZATION MODEL

The main source of heat needed to evaporate the cryogenic liquid that spills on land is heat energy stored in the ground. Initially, the heat transfer of the film boiling type, which is influenced by the vapor blanket formed between the liquid and the ground surface, dominates. However, as the ground surface temperature decreases, the vapor blanket disappears and nucleate boiling occurs, resulting in better thermal contact and faster heat transfer. Thus, conduction heat transfer through the ground controls the heat flux into the liquid pool. Based on these phenomena, we can make a vaporization model by adding the following assumptions: 1) only the heat source through the ground governs the vaporization, 2) the liquid pool is thin enough and the whole pool is at a uniform temperature equal to its boiling point, 3) the liquid pool is in perfect thermal contact with the ground, and 4) the conduction heat transfer from the ground to the liquid pool is one-dimensional in the direction of gravity.

By solving the one-dimensional heat conduction equation modeled by the above assumptions, the heat flux into the liquid pool is (Briscoe 1980)

$$q' = \frac{k(T_a - T_b)}{(\pi\alpha)^{0.5}} t^{-0.5}, \tag{1}$$

where $q'$ is heat flux, $k$ is thermal conductivity of the ground, $T_a$ is the ambient temperature, $T_b$ is the boiling point, $\alpha$ is thermal diffusivity of the ground, and $t$ is time. For a non-spreading pool where the pool area has not changed, the vaporization velocity is obtained as follows:

$$E_n = \frac{q'}{\rho L} = \frac{k(T_a - T_b)}{\rho L(\pi\alpha)^{0.5}} t^{-0.5}, \tag{2}$$

where $E_n$ is the vaporization velocity of the non-spreading pool, $\rho$ is density of the liquid, and $L$ is latent heat of vaporization.

Based on the vaporization velocity of the non-spreading pool shown in Eq. (2), the vaporized volume from the annular element of the spreading pool in Fig. 1 becomes

$$V = 2\pi r dr \cdot \frac{k(T_a - T_b)}{\rho L(\pi\alpha)^{0.5}} (t-\tau)^{-0.5}, \tag{3}$$

where $V$ is the vaporized volume, $r$ is radius, $\tau$ is the spreading time for the annular element to reach the radius $r$, the pool is assumed to be a circular cylinder, and $t$ is the arrival time of the spreading pool at radius $R$ from the origin where $t = 0$.

Then the vaporization velocity for the spreading pool with a radius $R$ is

$$E_s = \frac{1}{\pi R^2} \int_0^R V\, dr = \frac{1}{\pi R^2} \frac{k(T_a - T_b)}{\rho L(\pi\alpha)^{0.5}} \int_0^{R(t)} \frac{2\pi r dr}{(t-\tau)^{0.5}}, \tag{4}$$

where $E_s$ is the vaporization velocity for the spreading pool.

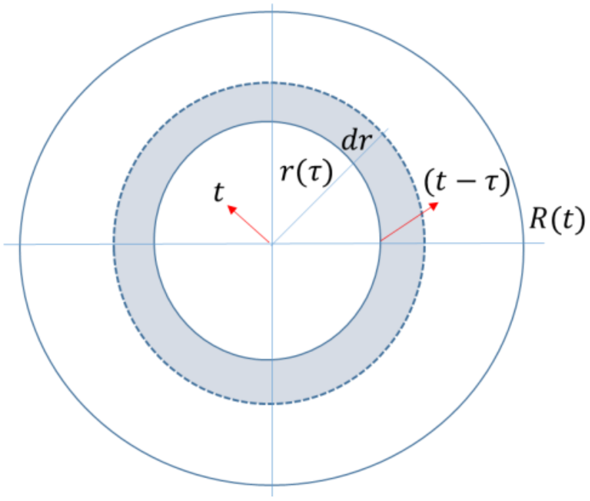


Fig. 1 Vaporization from the spreading pool

The vaporization velocity of the non-spreading pool may be determined quickly because it is a function of time alone as in Eq. (2). On the other hand, it is not straightforward to obtain the vaporization velocity for the spreading pool because it depends on both the time and pool area, and annular ground elements contact the liquid for different time periods as in Eq. (4). The vaporization velocity as a function of time $t$ only can be obtained if the spread data $r(\tau)$ are known. In the present work the spread data were measured using several thermocouples installed at specific intervals. Thus,

$$E_s = \frac{1}{\pi R^2}\frac{k(T_a - T_b)}{\rho L(\pi\alpha)^{0.5}}\left[\int_0^{R_1(t_1)} \frac{2\pi r dr}{(t-\tau)^{0.5}} + \int_{R_1(t_1)}^{R_2(t_2)} \frac{2\pi r dr}{(t-\tau)^{0.5}} +..+ \int_{R_{n-1}(t_{n-1})}^{R_n(t_n)} \frac{2\pi r dr}{(t-\tau)^{0.5}}\right], \tag{5}$$

where $R_1$ is the location of the nearest thermocouple from the center of the ground and $R_n$ is for the farthest thermocouple. If the measured radius can be assumed to be linear with time in each range as follows:

$$r(\tau) = c_1 + c_2\tau, \tag{6}$$

Eq. (5) can be integrated analytically using follows:

$$\int_{R_1(t_1)}^{R_2(t_2)} \frac{2\pi r dr}{(t-\tau)^{0.5}} = \int_{t_1}^{t_2} \frac{2\pi(c_1 + c_2\tau) d(c_1 + c_2\tau)}{(t-\tau)^{0.5}}$$
$$= -4\pi c_2\left[\sqrt{t-t_2}\left(\frac{2}{3}c_2 t + c_1 + \frac{1}{3}c_2 t_2\right) - \sqrt{t-t_1}\left(\frac{2}{3}c_2 t + c_1 + \frac{1}{3}c_2 t_1\right)\right], \tag{7}$$

## 3. EXPERIMENTAL SET UP

The cryogenic liquids used in the experiments are liquid nitrogen and liquid oxygen, and physical properties of them and of the concrete ground are shown in Table 1 and 2.

Table 1 Properties of liquid nitrogen and liquid oxygen at atmosphere (Wylen 1976)

| | Density ($kg/m^3$) | Latent heat of vaporization(kJ/kg) | Boiling temperature(K) |
|---|---|---|---|
| Liquid nitrogen | 808.4 | 198.6 | 77.3 |
| Liquid oxygen | 1140.9 | 212.9 | 90.1 |

Table 2 Properties of the concrete ground (Olewski 2013)

| Density, $kg/m^3$ | Thermal conductivity, W/(m-K) | Thermal diffusivity, $m^2/s$ |
|---|---|---|
| 2300 | 1.04 | $9.5\times10^{-7}$ |

The experimental apparatus consists of a digital balance, a liquid storage tank, thermocouples, and a data acquisition device as shown in Fig. 2. A digital balance with a resolution of 0.1 kg was used to measure the liquid weight in the storage tank under test. The release rate can be evaluated from the liquid weight over time. The liquid tank was well insulated to prevent heat transferred from the ambient to the liquid. The cryogenic liquid was released from the tank onto the center of the 3 m diameter concrete plate through a discharge nozzle. Four discharge nozzles with different inner diameters were used to obtain four different release rates. Four experiments were performed for each nozzle for a consistent experiment, and the estimated average release rates and release times are shown in Table 3. Thermocouples were distributed in two perpendicular directions, as shown in Fig. 3, to determine the arrival time of the pool front at predetermined locations. The thermocouples were held by thermocouple holders. In general, each thermocouple holder was able to hold 5 thermocouples. Twenty-three thermocouples were installed along each direction, and the distances of thermocouples with reference to the center of the concrete plate are given in Table 4. A thermocouple was installed in a manner that its tip had contact with the plate surface. The liquid pool was considered to spread to a thermocouple location if the temperature measured by the thermocouple dramatically dropped to the boiling point of the liquid. The data acquisition system simultaneously recorded data obtained from the digital balance and thermocouples.

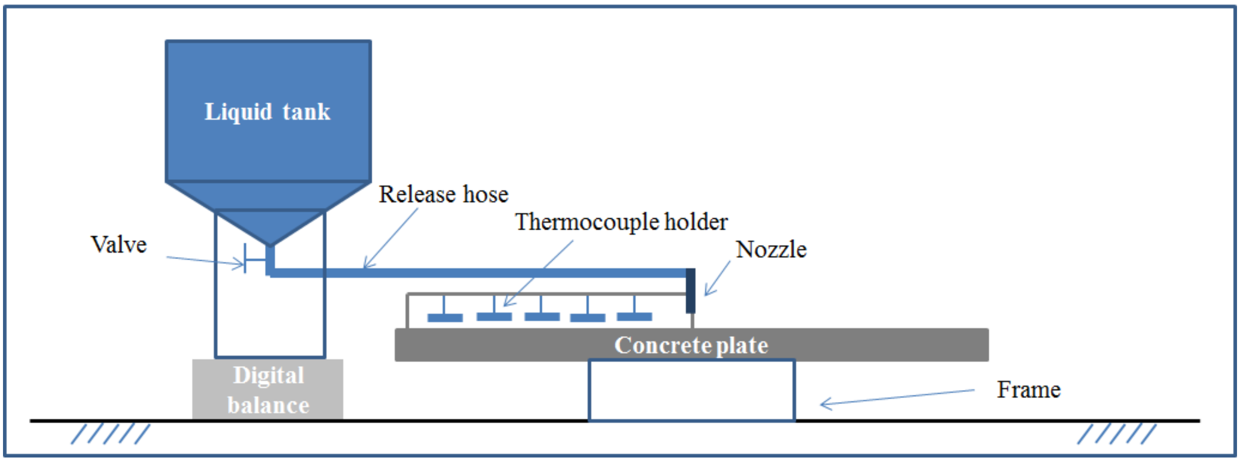


Fig. 2 General schematic layout of the experimental apparatus

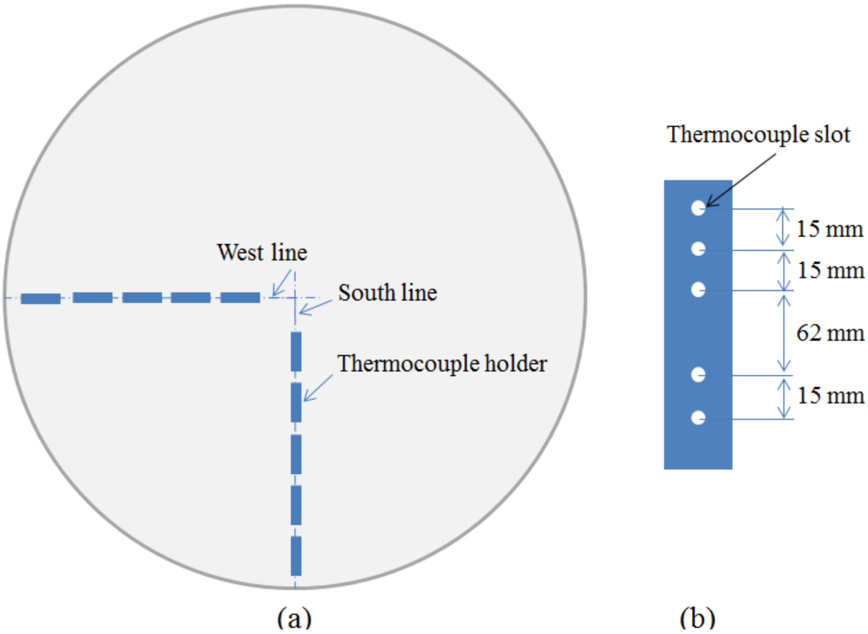


Fig. 3 Thermocouple distribution (a) General schematics (b) Thermocouple holder's detail

Table 3 Release rate and time

| Nozzle Diameter, mm | Liquid nitrogen | | | Liquid oxygen | | |
|---|---|---|---|---|---|---|
| | Release rate | | Release time, s | Release rate | | Release time, s |
| | kg/s | $\times 10^{-4}$ $m^3/s$ | | kg/s | $\times 10^{-4}$ $m^3/s$ | |
| 6 | 0.045±0.005 | 0.558±0.062 | 1717±155 | 0.069±0.001 | 0.605±0.006 | 1214±15 |
| 10 | 0.072±0.002 | 0.893±0.025 | 1071±33 | 0.115±0.003 | 1.004±0.023 | 741±21 |
| 14 | 0.147±0.002 | 1.824±0.025 | 522±7 | 0.226±0.022 | 1.981±0.193 | 373±39 |
| 18 | 0.276±0.016 | 3.424±0.198 | 277±17 | 0.383±0.017 | 3.359±0.153 | 232±11 |

Table 4 Thermocouple location

| Thermocouple | Distance from the plate center, m | Thermocouple | Distance from the plate center, m |
|---|---|---|---|
| West_No1, South_No1 | 0.204 | West_No13, South_No13 | 0.734 |
| West_No2, South_No2 | 0.219 | West_No14, South_No14 | 0.796 |
| West_No3, South_No3 | 0.234 | West_No15, South_No15 | 0.811 |
| West_No4, South_No4 | 0.296 | West_No16, South_No16 | 0.954 |
| West_No5, South_No5 | 0.311 | West_No17, South_No17 | 0.969 |
| West_No6, South_No6 | 0.454 | West_No18, South_No18 | 0.984 |
| West_No7, South_No7 | 0.469 | West_No19, South_No19 | 1.046 |
| West_No8, South_No8 | 0.484 | West_No20, South_No20 | 1.061 |
| West_No9, South_No9 | 0.546 | West_No21, South_No21 | 1.204 |
| West_No10, South_No10 | 0.561 | West_No22, South_No22 | 1.234 |
| West_No11, South_No11 | 0.704 | West_No23, South_No23 | 1.311 |
| West_No12, South_No12 | 0.719 | | |

## 4. RESULTS AND DISCUSSION

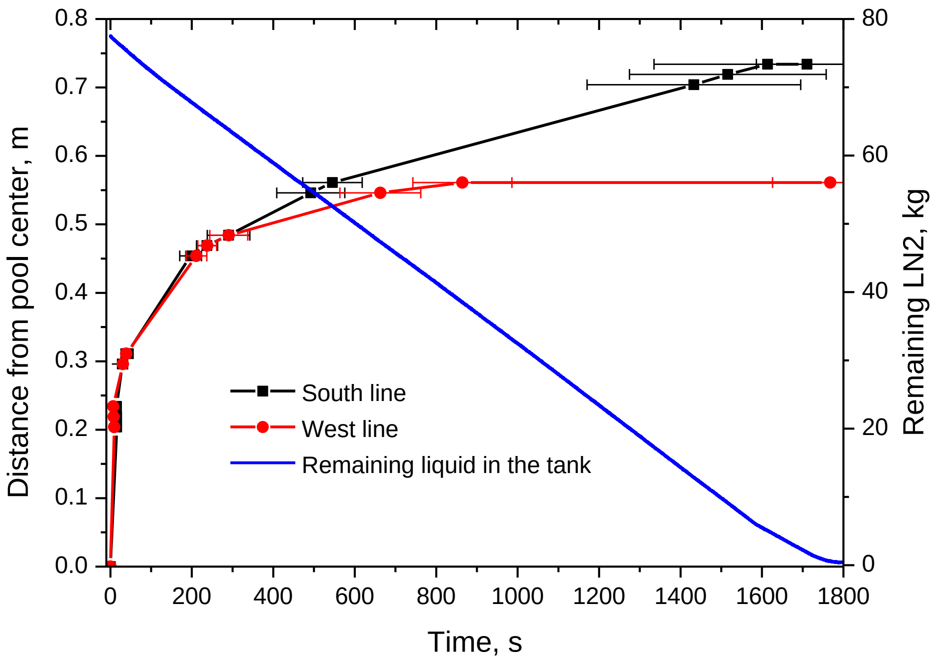


Fig. 4 Spread data for the 6 mm nozzle

The experiment was repeated 4 times for the same nozzle. As shown in Fig. 4, the spread rates in two directions are almost the same at the initial stage of spread, but the spread rate in the south direction is larger when the distance is more than 0.5 m. In addition, it can be seen that the error range of the data, that is, the standard deviation, also increases in the late period of spread. It is also seen that the spill rate is almost constant during the experiment from the weight of the liquid remaining in the storage tank. This non-uniform spread is due to the difficulty of producing a precise concrete plate, and therefore it is assumed that this spread is elliptical for data processing. To obtain the circular spread corresponding to this elliptical one, equivalent radius was introduced as follows: $R(t) = \sqrt{ab}$, where $R$ is the equivalent circular pool radius, and as shown in Fig. 5, $a$ and $b$ are the mean values of the boundary positions of the elliptical pool obtained in the 4 replicate experiments. $a$ and $b$ could be determined by linear interpolation using neighboring experimental data of pool boundary along West and South lines.

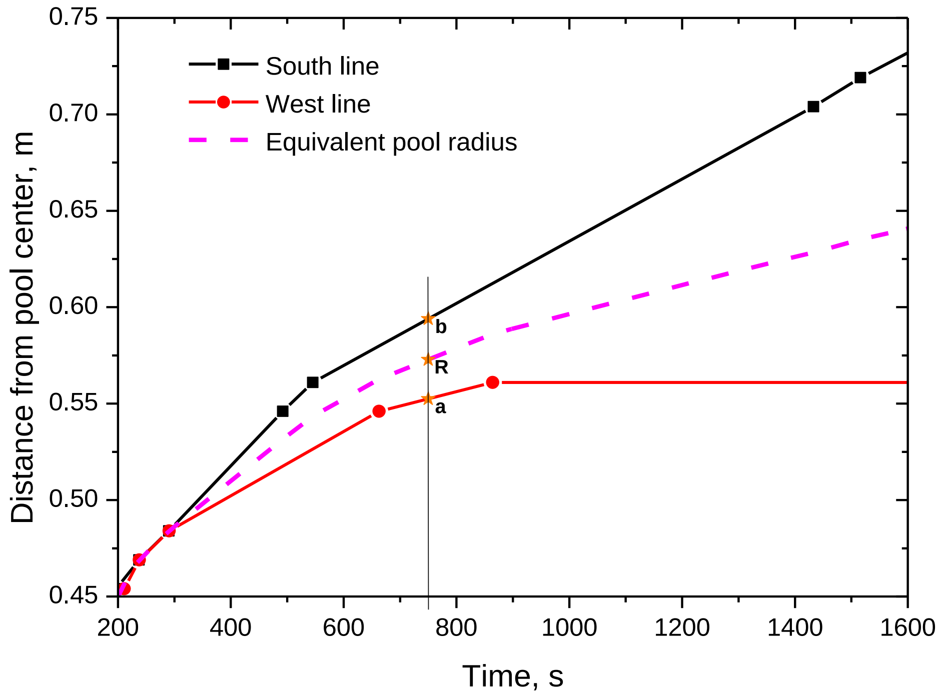


Fig. 5 Equivalent radius for the 6 mm nozzle

The spread of liquid nitrogen and liquid oxygen using the equivalent radii defined above is shown in Figs. 6-7. It can be seen that the average spread rate increases as the release rate increases for both liquids, which is due to the increase in inertia force with increasing release rate (Nguyen 2017). The reason why the spread rate of liquid oxygen is slightly larger than that of liquid nitrogen is due to the difference in the release rate of both fluids. As shown in Table 3, for the same nozzle the release rate of liquid nitrogen is smaller than that of liquid oxygen.

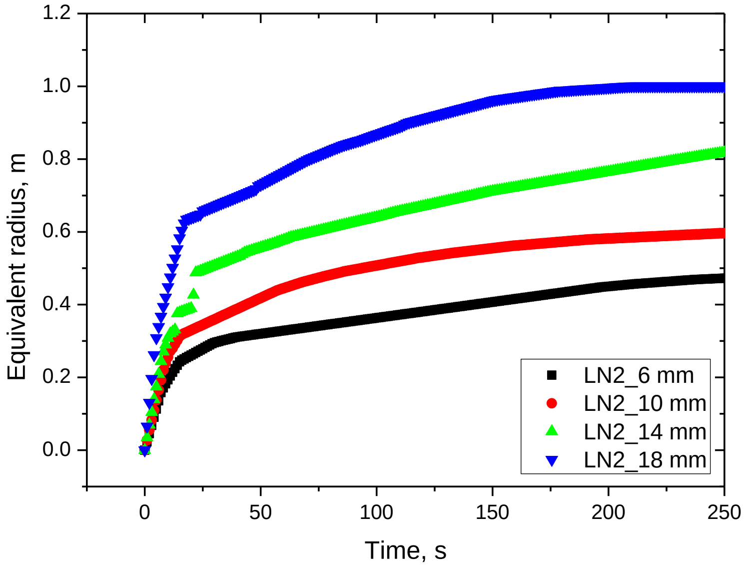


Fig. 6 The equivalent radius for liquid nitrogen

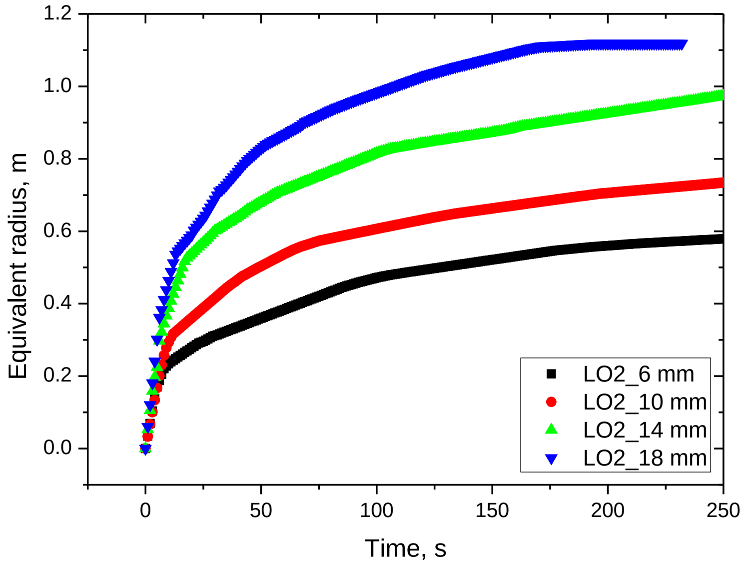


Fig. 7 The equivalent radius for liquid oxygen

The vaporization velocity versus pool radius was calculated for both liquid nitrogen and liquid oxygen using the methodology described in section 2. The methodology required the pool radius to be a linear function of time. Therefore, the equivalent radius curve was divided into approximated linear sections. The distance between two calculation points was 0.05 m. The results are shown in Figs. 8-9. The vaporization velocity was calculated from the pool radius of 0.2 m to 0.6 m and 0.75 m for liquid nitrogen and liquid oxygen, respectively. Those are the maximum pool radius of the case with the smallest release rate. The case with nozzle diameter D = 14 mm shows abnormal results at pool radius of 0.45 m and 0.3 m for liquid nitrogen and liquid oxygen, respectively, which are opposed to the other cases. The abnormality is not considered a physical behavior. It can be seen that the greater the release rate, the higher the vaporization velocity. This can be explained by investigating the contact time of an annular ground element with fast and slow-spreading pools when the pools spread to a pre-determined radius. As the release rate increases, the pool spreads faster. When both pools spread to the same radius, the contact time of an annular ground element with the liquid in case of the fast-spreading pool is shorter than that of the slow-spreading pool. Therefore, the vaporization velocity of the fast-spreading pool is higher than that of the slow-spreading pool, as can be seen in Eq. (5). In addition, the vaporization velocity decreases with the pool radius.

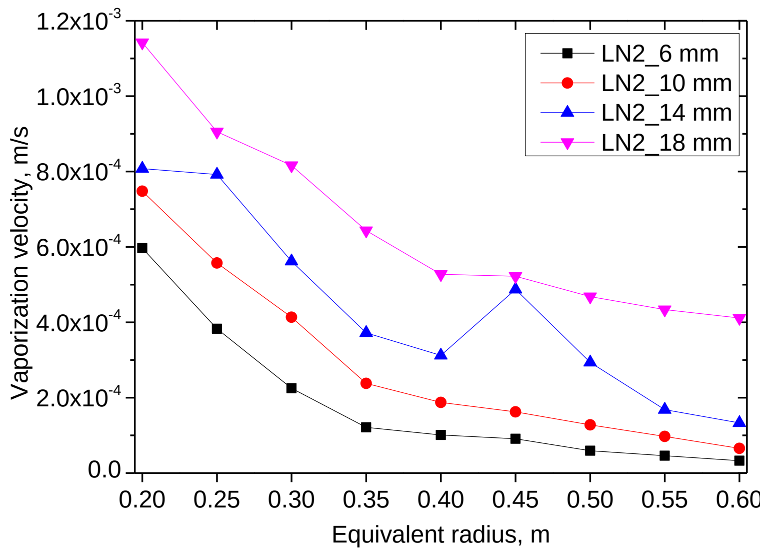


Fig. 8 Vaporization velocity versus pool radius for liquid nitrogen

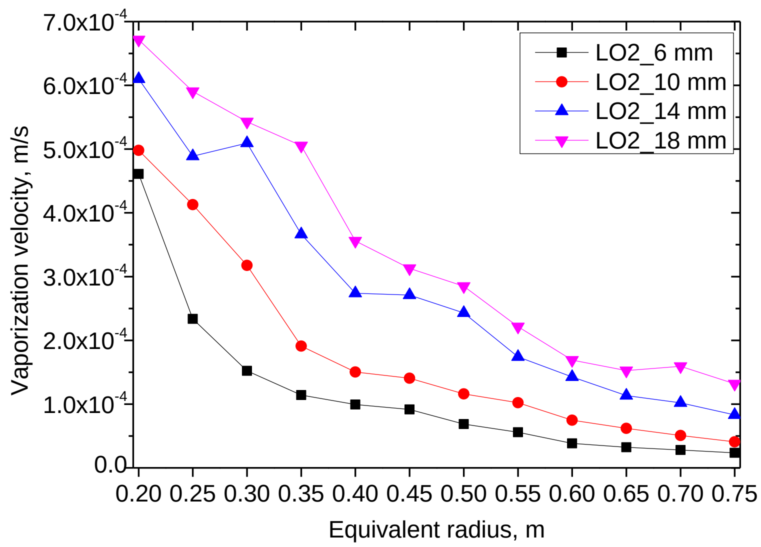


Fig. 9 Vaporization velocity versus pool radius for liquid oxygen

The vaporization velocity versus time is shown in Figs. 10-11 for liquid nitrogen and liquid oxygen, respectively. It can be seen that the vaporization velocity decreases with time. The vaporization velocity of a spreading pool is higher than that of a non-spreading pool. This is because the spreading pool can receive heat from new warm ground. The effect of the release rate on the vaporization velocity versus pool radius was clearly seen. However, it is difficult to distinguish the effect of the release rate on the vaporization velocity versus time. This is due to the fact that the differences of the release rate among the cases are not significant enough to recognize the effect.

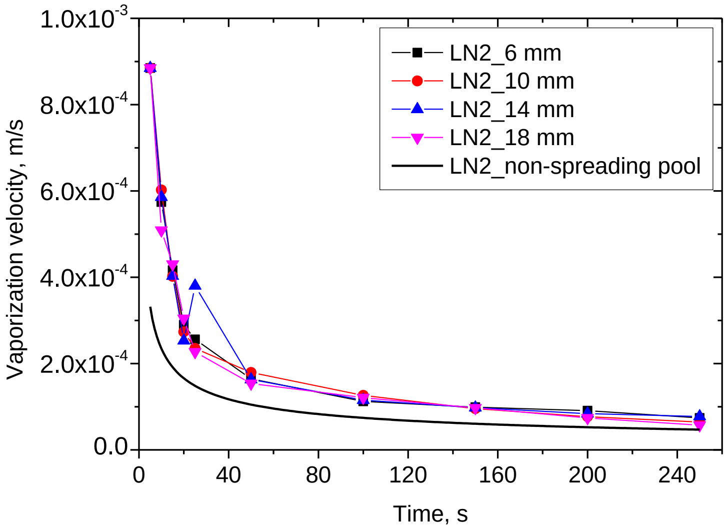


Fig. 10 Vaporization velocity versus time for liquid nitrogen

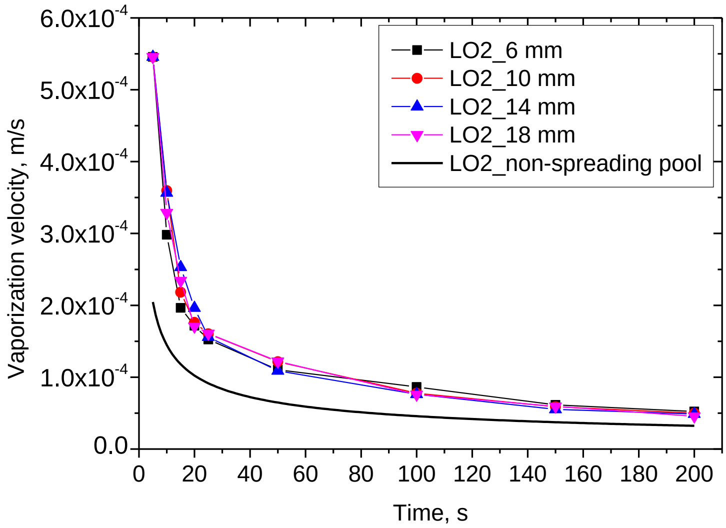


Fig. 11 Vaporization velocity versus time for liquid oxygen

## 5. CONCLUSIONS

In this work, experiments of spreading and vaporization of liquid nitrogen and liquid oxygen on the concrete ground were conducted. Pool radius with time was the only measured parameter. A semi-analytical model was derived based on the solution of the 1-D unsteady heat conduction equation. Then the vaporization velocity was evaluated based on the semi-analytical model using pool spread data. The model does not require the information of the release rate and pool mass. The results indicated that a greater release rate results in a faster-spreading pool, which in turn increases the vaporization velocity versus pool radius. However, the effect of the release rate on the vaporization velocity versus time in the experimental cases was not seen due to the small range of release rate. And the vaporization velocity decreases with both the pool radius and time.

## REFERENCES

Briscoe, F. and Shaw, P. (1980), “Spread and evaporation of liquid”, *Prog. Energy Comb Sci.*, **6**, 127-140.

Kim, M., Do, K., Choi, B. and Han, Y. (2012), “High-order perturbation solutions to a LH2 spreading model with continuous spill”, *International Journal of Hydrogen Energy*, **37**(22), 17409-17414.

Verfondern, K. and Dienhart, B. (1997), “Experimental and theoretical investigation of liquid hydrogen pool spreading and vaporization”, *International Journal of Hydrogen Energy*, **22**(7), 649-660.

Brandeis, J. and Kansa, E.J. (1983), “Numerical simulation of liquefied fuel spill: I. Instantaneous release into a confined area”, *International Journal for numerical methods in fluid*, **3**, 333-345.

Brandeis J. and Ermak D.L. (1983), “Numerical simulation of liquefied fuel spills: II. Instantaneous and continuous LNG spills on an unconfined water surface”, *International Journal for numerical methods in fluid*, **3**, 347-361.

Stein, W. and Ermak, D.L. (1980), “One-dimensional numerical fluid dynamic model of spreading of liquefied gaseous fuel (LGF) on water”, *Lawrence Livermore National Laboratory Report* No. UCRL-53078.

Webber, D.M. (1990), “A model for pool spreading and vaporization and its implementation in the computer code GASP”, *SRD/HSE Report* No. R507.

American Petroleum Institute (2008), “Consequence analysis in an API RBI assessment”, *API RP 581 PART 3*, Washington, D. C., USA, Section 5.5.

Zabetakis, M.G. and Burgess, D.S. (1960), “Research on the hazard associated with the production and handling of liquid hydrogen”, *WADD Technique Report*.

Takeno, K., Ichinose, T., Hyodo, Y. and Nakamura, H. (1994), “Evaporation rates of liquid hydrogen and liquid oxygen spilled onto the ground”, *Journal of Loss Prevention in the Process Industries*, **7**(5), 425-431.

Olewski, T., Vechot, L. and Mannan, S. (2013), “Study of the Vaporization Rate of Liquid Nitrogen by Small and Medium-Scale Experiments”, *The Italian Association of Chemical Engineering*, **31**, 133-138.

Reid, R.C. and Wang, R. (1978), "The boiling rate of LNG on typical dike floor materials", *Cryogenics*, **18**, 401-404.

Kim, M., Nguyen L. and Choi, B. (2016), "Experimental study of the evaporation of spreading liquid nitrogen", *Journal of Loss Prevention in the Process Industries*, **39**, 68-73.

Nguyen, L., Kim, M. and Choi, B. (2017), "An experimental investigation of the evaporation of cryogenic-liquid-pool spreading on concrete ground", *Applied Thermal Engineering*, **123**, 196-204.

Wylen, G.J. Van and Sonntag, R.E. (1976), "Fundamentals of classical thermodynamics", *John Wiley and Sons*, New York, 674-677.